HHS Public Access

Author manuscript

Clin Sci (Lond). Author manuscript; available in PMC 2021 February 13.

Published in final edited form as:

Clin Sci (Lond). 2020 July 17; 134(13): 1763–1774. doi:10.1042/CS20200184.

Ctcf is Required for Renin Expression and Maintenance of the Structural Integrity of the Kidney

Maria Florencia Martinez[1,2], **Alexandre G. Martini**[1,2], **Maria Luisa S. Sequeira-Lopez**[1,2,3], **R. Ariel Gomez**[1,2,3]

[1]Child Health Research Center, University of Virginia School of Medicine, Charlottesville, Virginia, 22908. United States.

[2]Department of Pediatrics, University of Virginia School of Medicine, Charlottesville, Virginia, 22908. United States.

[3]Department of Biology, University of Virginia School of Medicine, Charlottesville, Virginia, 22908. United States.

Abstract

Renin cells are crucial for the regulation of blood pressure and fluid electrolyte homeostasis. We have recently shown that renin cells possess unique chromatin features at regulatory regions throughout the genome that may determine the identity and memory of the renin phenotype. The 3-D structure of chromatin may be equally important in the determination of cell identity and fate. CCCTC-binding factor *(Ctcf)* is a highly conserved chromatin organizer that may regulate the renin phenotype by controlling chromatin structure. We found that *Ctcf* binds at several conserved DNA sites surrounding and within the renin locus, suggesting that *Ctcf* may regulate the transcriptional activity of renin cells. In fact, deletion of *Ctcf* in cells of the renin lineage led to decreased endowment of renin-expressing cells accompanied by decreased circulating renin, hypotension, and severe morphological abnormalities of the kidney, including defects in arteriolar branching, and ultimately renal failure. We conclude that control of chromatin architecture by *Ctcf* is necessary for the appropriate expression of renin, control of renin cell number and structural integrity of the kidney.

Keywords

renin; hypertension; renin-angiotensin system

Correspondence: R. Ariel Gomez, MD, Harrison Distinguished Professor of Pediatrics and Biology, Director, Child Health Research Center, Director, Center of Excellence in Pediatric Nephrology, 409 Lane Road, Rooms 2001, 2006, 2010. Charlottesville, VA, 22908, rg@virginia.edu, Phone: 434 924 2525, Fax: 434 982 4328.

Authors Contribution

RAG conceived and directed the project. MFM, RAG, MLSSL conceived the experiment design. MFM, AM, performed experiments and contributed to the manuscript. MFM and AM analyzed and interpreted data. RAG and MLSSL. MFM and RAG wrote the manuscript with the contribution of all the authors. RAG and MLSSL supervised the research.

Conflict of interest: The authors have declared that no conflict of interest exists.

Subjects:

Cardiovascular System & Vascular Biology; Molecular Bases of Health & Disease

INTRODUCTION

Renin-expressing cells are fundamental for the maintenance of extracellular fluid volume, blood pressure homeostasis. Through evolution, these cells have acquired additional roles in kidney vascular development, regeneration and innate immune defense[1,2]. In adult mammals, renin-expressing cells are localized to the walls of the afferent arterioles at the entrance to the glomeruli[3]. These juxtaglomerular (JG) cells synthesize and release the enzyme/hormone renin in response to changes in blood pressure and extracellular fluid volume. We have recently shown that renin cells possess unique chromatin features at regulatory regions throughout the genome that determine the identity and memory of the renin phenotype[4]. A group of these regulatory regions denominated as super-enhancers are characterized by high levels of histone 3 lysine 27 acetylation (H3K27ac), a histone mark associated with active enhancers, open chromatin as determined by ATAC-seq, and high levels of transcription factor binding such as deposition of the Mediator subunit 1 (*Med1*)[4] as determined by Chip-Seq, and high transcriptional activity of the genes they regulate as it is the case with the renin gene in native and tumoral renin-expressing cells[4]. In addition to the aforementioned layer of regulation, the 3D organization of chromatin may be crucial in determining the fate of renin cells during development and disease. Within the cell nucleus, the chromatin is packed in chromosomal territories which are compartmentalized by the formation of topological associated domains (TADS) that are delimitated by the CCCTC-binding factor (*Ctcf*), the best-characterized chromatin architectural protein[5]. *Ctcf* is a DNA binding factor localized at chromosome 8 on the mouse genome that plays an essential role in the regulation of gene expression. *Ctcf* is an 11-zinc finger protein, highly conserved among vertebrates, that binds numerous intergenic sites genome-wide regulating transcriptional activity through the different combinations of its zinc fingers[6,7]. Initially, *Ctcf* was discovered as a transcriptional repressor of the *Myc* gen[8], but it has other significant regulatory functions, for example as a transcriptional activator or repressor, as an insulator acting as a barrier preventing undesired gene activation[9] and mediating long-range chromatin interactions bringing into proximity enhancers to the promoter of target genes[10].

Because our general interest is to understand how the chromatin is organized to regulate the renin phenotype, we sought to determine whether *Ctcf* is involved in the regulation of renin and the maintenance of the renin phenotype *in vivo*. Conditional loss of *Ctcf* in cells from the renin lineage resulted in a decrease endowment of renin-expressing cells accompanied by decreased circulating renin, hypotension, severe renal abnormalities and ultimately renal failure. Results indicate that *Ctcf* is necessary for the control of renin cell number, renin expression and the structural integrity of the kidney.

Experimental Methods

Animals.—*Ctcf floxed* mice were obtained from Niels Galjart from the Erasmus Medical Center in the Netherlands[11]. To investigate the function of *Ctcf* in renin-expressing cells we

bred *Ctcf*$^{fl/fl}$ with *Ren1*$^{dCre/+}$ expressing *Cre recombinase* in renin cells[12]. After a few generations, we generated *Ctcf*$^{fl/fl}$; *Ren1*$^{dCre/+}$ conditional knock-out mice and *Ctcf*$^{fl/fl}$; *Ren1*$^{d+/+}$ as control mice. Mice were studied at 1, 2 and 4 months of age. Males and females were used for this study. Although the dispersion of the data seemed to indicate that there was not statistical difference between males and females, we did not have sufficient numbers of animals in either sex limiting our statistical power to detect differences between the sexes. Therefore, animals from both sexes were grouped to perform statistics and to display the data. All the animal experiments were performed in the Pediatric Center of Excellence in Nephrology at the University of Virginia.

All animals were handled following the National Institutes of Health guidelines for the care and use of experimental animals, and the study was approved by the Institutional Animal Care and Use Committee of the University of Virginia.

Genotyping.—Mouse genotypes from tail biopsies were determined using real-time PCR with specific probes designed by Transnetyx, Cordova, TN.

Cell Culture.—As4.1 renin expressing cell line (ATCC® CRL-2193TM)[13], was cultured in high glucose DMEM (Gibco #11965–092) + 10% FBS at 37°C in a humidified incubator containing 5% of CO2.

Chromatin Immunoprecipitation Assay.—ChIP was performed in As4.1 cells using the ChIP-IT High Sensitivity® (HS) Kit (Cat. No. 53040; Active Motif, Carlsbad, CA, USA) and ChIP-IT® qPCR Analysis Kit (Cat. No. 53029; Active Motif, Carlsbad, CA, USA) following the manufacturer's protocol and using a polyclonal antibody against CTCF (Cat. No. 07–729, Millipore). Quantitative real-time PCR amplification was performed using SsoAdvanced SYBR® Green Supermix (Cat. No. 172–5260, Bio-Rad Laboratories, Inc, CA, USA) and 5 μL of DNA sample. Specific primers were designed to detect *Ctcf* binding sites at the neighborhood of the mouse *Ren1* gene. The program we used to quantify the amplification was 2 min at 98 °C, 5 s at 98 °C, 15 s at 58 °C for 40 cycles in 20 μL reaction volume. Data were plotted and presented in the form of a histogram.

RNA extraction and Quantitative Real-Time PCR.—Whole kidneys from control and mutant mice were removed and placed in RNA*later* (Ambion, Austin, TX) overnight at 4°C and then stored at −20°C. Total RNA was isolated using TRIzol extraction (Life Technologies, Grand Island, NY) according to the manufacturer's instructions. cDNA was prepared from 3μg of RNA using Maloney murine leukemia virus reverse transcriptase (Promega) and an oligo(dT) primer according to the manufacturer's instructions. Quantitative reverse transcription polymerase chain reaction (RT-PCR) was performed using SYBR Green I (Invitrogen Molecular Probes, Eugene, OR) in a CFX Connect system (BioRad, Hercules, CA). *Ren1* mRNA expression was normalized to *S14* expression, and the changes in expression were determined by the ΔΔCt method and the reported as relative expression compared to control mice. The following gene-specific primers were used: *Ren1*, forward, 5'- ACAGTATCCCAACAGGAGAGACAAG-3', reverse, 5'-GCACCCAGGACCCAGACA −3'; *S14*, forward, 5'-CAGGACCAAGACCCCTGGA-3', reverse 5'-ATCTTCATCCCAGAGCGAGC-3'.

Histological and immunohistochemical analysis.—Mice were anesthetized with tribromoethanol (300 mg/kg). Kidneys were harvested at indicated time points, weighed, and either fixed in 2% paraformaldehyde (PFA) for 1 hour at 4°C for frozen sections or fixed overnight in Bouin's or formalin fixative, and embedded in paraffin. Sections (5–10 μm) from paraffin-embedded or cryo-fixed tissues were used for histological analysis. Bouin's fixed paraffin kidney sections were deparaffinized in xylenes and graded alcohols and stained with Hematoxylin and Eosin to examine overall kidney morphology. Masson's Trichrome was performed to identify areas of fibrosis as described previously[14,15]. We performed immunohistochemistry for renin (1:500 dilution of rabbit polyclonal anti-mouse antibody)[14] to determine the distribution of renin-expressing cells and α-smooth muscle actin (SMA, 1: 10,000 dilution of mouse monoclonal antibody; Sigma, St.Louis, MO) to evaluate vascular architecture, as described previously[16,17]. The juxtaglomerular apparatus (JGA) index was calculated as the number of renin-positive JGA per total number of glomeruli and expressed as a percentage[4,18]. Immunostaining using DAB was performed with the appropriate Vectastain ABC kits (Vector Laboratories, Burlingame, CA).

Blood Pressure Measurement.—Mice at 4 months of age were anesthetized with 1.5% isoflurane and placed on a thermostatically controlled heating table at 37.5°C. A polyethylene catheter (Becton Dickinson) pre-filled with heparinized saline was inserted into the right carotid so that the catheter tip lied at the aortic root. Mean arterial pressure was continuously recorded from this catheter by means of an RX104A transducer coupled to a data acquisition system and AcqKnowledge software (Biopac Systems, Inc.). Measurements of mean arterial pressure, systolic and diastolic blood pressure were taken over a 10-min period[19,20]. Animals were euthanized after the procedure.

Blood Chemistry.—Blood was collected by cardiac puncture or through the carotid catheter when mice were subjected to blood pressure measurement. After blood was collected for renin measurements, blood samples were collected into heparinized and EDTA plasma separator tubes (Microtainer). Complete blood count and the basic metabolic panel were performed by the University of Virginia Hospital clinical laboratory.

Plasma renin.—Plasma renin concentration was determined using ELISA following the manufacturer's instructions (RayBiotech, Norcross, GA).

Renal arterial tree micro-dissection.—Kidneys attached to the aorta were harvested from 4 months old mice and incubated in 6 M hydrochloric acid for one hour followed by several washes with acidified water (pH 2.5), as we previously described[21,22]. The arterial trees were carefully dissected and imaged under a stereomicroscope for counting the arteriolar branches.

Statistics.—Number of animals studied and statistical parameters are reported in each of the figures and figure legends. Results statistically significant were obtained when $p < 0.05$ by two-tailed Student's t-test or ANOVA. Statistical analysis was performed in GraphPad Prism 8.

RESULTS

Ctcf binds to the renin locus and surrounding domains in renin cells

To investigate whether *Ctcf* binds at the *Ren1* locus, we first inquired into published data generated by the ENCODE project[23]. Figure 1A shows the binding of *Ctcf* within the neighborhood of the *Ren1* gene in different mouse tissues and cell types. The pervasiveness of these binding sites in intergenic and intronic regions at this locus, suggest that *Ctcf* may play a role as a general chromatin organizer of this genomic region (Figure 1A). These binding sites were also identified in other species (data not shown)[23], indicating that these sites are highly conserved throughout evolution. To define the distribution of *Ctcf* binding in renin-expressing cells, we performed chromatin immunoprecipitation followed by qPCR (ChIP-qPCR) to identify either new sites, or to verify the *Ctcf* binding sites mentioned above at the *Ren1* locus in As4.1 cells in culture[13]. As mentioned above, As4.1 cells are constantly producing and secreting renin from the $Ren1^c$ gene, and as we have recently published they shared with the native renin cells isolated from mice, the same chromatin pattern and a set of unique super-enhancers that control renin cell identity[4]. ChIP-qPCR results in As4.1 cells showed that the binding enrichment of *Ctcf* (at *Ctcf* binding sites) exceeds 5-fold with respect to the negative region tested which also has a low background, evidenced by the binding events detected per 1,000 cells below a value of 2 (Figure 1B). We detected *Ctcf* signal enrichment in regions that coincide with the areas mentioned above and found in ENCODE: upstream the coding region of the renin gene, within intron one and between *Etnk2* and *Sox13* (Figure1B, green dashed lines). Only one binding area for *Ctcf* in kidney tissue sample did not show an enrichment in As4.1 cells (Figure 1B, pink dashed line) which could be tissue specific, although its function remains to be determined. Overall, these results indicate that *Ctcf* binds within and around the renin locus and might be involved in renin regulation by controlling chromatin architecture.

Deletion of Ctcf in renin cells results in decrease renin mRNA levels, circulating renin, and arterial blood pressure.

Because homozygous deletion of *Ctcf* results in embryonic lethality[24], we generated mice with conditional deletion of *Ctcf* in cells of the renin lineage by crossing *floxed Ctcf* mice[11] with mice expressing *Cre* recombinase under the control of the $Ren1^d$ promoter (*Ctcf-cKO*)[15] (Supplementary Figure 1). Throughout fetal and early postnatal life during vascular development, renin precursor cells differentiate into smooth muscle cells, mesangial cells, and interstitial pericytes[12]. Thus, *Ctcf* in our mouse model is deleted throughout the renal arterial tree, in all cells that had ever expressed renin. We studied *Ctcf-cKO* mice at 4 months of age. Deletion of *Ctcf* in renin cells *in vivo* caused an 80% reduction of relative renin mRNA levels in comparison with control mice (0.231 ± 0.046 *vs.* 1.04 ± 0.103; $p<0.0001$, Figure 2A). In addition, circulating plasma renin was significantly decreased in *Ctcf*-cKO versus control mice (15,277 ± 2,562 *vs.* 62,322 ± 8,933 pg/mL; $p<0.001$, Figure 2B). Consistent with these results, *Ctcf*-cKO mice exhibited a significantly lower mean arterial blood pressure than control mice (60.09 ± 1.10 *vs.* 75.07 ± 1.25 mmHg, $p<0.0001$), Figure 2C.

Deletion of Ctcf causes severe depletion of renin cells.

Figure 3A shows renin immunostaining revealing fewer renin positive juxtaglomerular areas in *Ctcf-cKO* mice when compared to control mice. A way to quantitate the decreased in renin staining is calculating the juxtaglomerular index (JGI), which is the number of renin positive JG areas ÷ total number of glomeruli × 100[4,18]. *Ctcf*-cKO kidneys have a severely decreased JG index in comparison with control mice (9.69 ± 1.65 *vs.* 49.62 ± 2.91%; *p<0.0001*, Figure 3B).

Loss of Ctcf affects the branching pattern of the renal arterial tree.

Since renin cells are associated with the maturation of the renal vasculature, participating in the branching and elongation of the renal arterial tree, we wanted to investigate whether deletion of *Ctcf* in our mouse model also affects the kidney vasculature. We performed kidney arterial tree microdissections in both control and mutant mice[21]. As shown in Figure 4A, the arterial tree in *Ctcf-cKO* mice shows fewer branches than in control mice. Further, counting of arteriolar branching order revealed that mutant mice possess a reduced number of smaller arteries when compared with control mice which show a more extensive branching in the outer cortical region of the kidney (Figure 4B). Immunostaining for renin after vascular tree microdissection also showed fewer renin positive spots at the tip of afferent arterioles in *Ctcf-cKO* kidneys (Figure 4C).

Deletion of Ctcf in renin cells affects somatic and kidney growth and leads to kidney abnormalities.

The kidneys from 4-month-old *Ctcf-cKO* mice were, small, pale, and hard, displaying an irregular granular surface with areas of cortical depressions underlying morphological abnormalities and fibrosis (Figure 5A). *Ctcf*-cKO mice had lower body weights than control mice (20.91 ± 0.84 *vs* 25.15 ± 1.51g; *p<0.05*, Figure 5B). Moreover, the kidney/body weight ratio was markedly decreased in *Ctcf*-cKO mice indicating a more pronounced effect in the kidney than on somatic growth (1.032 ± 0.037 *vs.* 1.27 ± 0.032; *p< 0.001*, Figure 5C).

Hematoxylin staining of *Ctcf-cKO* kidneys revealed a disorganized kidney structure and lack of cortical-medullary demarcation, dilated tubules and proliferative tissue as evidenced by the large basophilic areas with numerous nuclei indicating areas of proliferation. These abnormalities were not present in control mice (Figure 5D). Masson's trichrome staining evidenced multiple fibrotic areas with increased collagen fibers (colored in blue) in kidneys of *Ctcf-cKO* mice coinciding with the cortical depressions mentioned above (Figure 5E, left). These areas of sclerosis were also observed surrounding the glomeruli and within glomeruli expanding the mesangium and reducing capillary lumens. Periodic Acid-Schiff-stained kidneys showed dilated tubules with intraluminal casts, and areas with crowded sclerotic glomeruli with extra-capillary hypercellularity and crescent glomeruli, as evidenced by the proliferating epithelial cells in the Bowman's space (Figure 5E, middle). Glomeruli also showed global thickened basement membranes and were surrounded by disorganized packed cells (Figure 5E, middle). Immunostaining for alpha-smooth muscle actin (αSMA) revealed active fibrotic processes in the kidneys of *Ctcf-cKO* mice indicated by interstitial cells expressing αSMA as well as cells surrounding and within the sclerotic glomeruli (Figure 5E, right).

Deletion of Ctcf leads to kidney failure.

Ctcf-cKO mice present chronic normocytic anemia characterized by low hemoglobin (9.773 ± 0.473 *vs.* 12.88 ± 0.289 g/dL; $p<0.001$, Figure 6A) and low hematocrit (37.18 ± 1.77 *vs.* 48.24 ± 1.18%; $p<0.001$, Figure 6B). In addition, blood urea nitrogen was increased in *Ctcf-cKO* mice when compared to control animals indicating renal failure (40.09 ± 4.699 *vs.* 24.29 ± 2.327mg/dL; $p<0.05$, Figure 6C). Moreover, measurement of urine osmolality indicated that *Ctcf-cKO* mice could not concentrate their urine appropriately (445.8 ± 36.21 *vs.* 1593 ± 165.5 mOSM/Kg; $p<0.0001$, Figure 6D).

Renin production is impaired in Ctcf-cKO mice at early stages.

To investigate when the phenotype described above for the deletion of *Ctcf* begins we studied mice at earlier stages, at 2 and 1 months of age. Macroscopically, at 2 months, kidneys of *Ctcf-cKO* mice have a normal shape and reddish appearance similar to the control group (Supplementary Figure 2A). We found no differences in somatic or kidney weight of *Ctcf-cKO* mice when compared to control mice (Supplementary Figure 2B–C). Histology of the kidneys showed a variable phenotype between mice showing focal areas of disorganized tissue structure (Supplementary Figure 2D). PAS staining evidenced focal areas with dilated tubules with the presence of casts and thickening of the glomeruli basement membrane (Supplementary Figure 2E, left). Masson trichrome performed in kidneys from *Ctcf-cKO* mice showed fibrosis in the interstitium as well as around and within glomeruli (Supplementary Figure 2E, middle). Immunostaining for αSMA revealed an increase of signal in the interstitium and surrounding glomeruli (Supplementary Figure 2E, right). Although positive areas for renin were encountered in *Ctcf-cKO* mice (Supplementary Figure 3A), the JG index revealed a reduced percentage of positive juxtaglomerular areas compared with control mice (22.5 ± 4.05 *vs.* 43.4 ± 6.2%, $p<0.001$; Supplementary Figure 3B) that was accompanied by a decreased in relative renin mRNA levels measured in kidney cortices of *Ctcf-cKO* mice (0.34 ± 0.11 *vs.* 1.07 ± 0.17, $p<0.01$; Supplementary Figure 3C). In addition, circulating plasma renin measured by ELISA was significantly decreased in *Ctcf*-cKO versus control mice (12,280 ± 2,049 *vs.* 36,692 ± 4,135 pg/mL; $p<0.0001$, Supplementary Figure 3D). Furthermore, we observed that *Ctcf-cKO* mice at 2 months of age were not able to concentrate their urine (407.9 ± 74.13 *vs.* 933.3 ± 124.1 mOSM/Kg, $p<0.01$; Supplementary Figure 3E).

On the other hand, at 1 month of age, we did not find macroscopic differences between *Ctcf-cKO* and control kidneys, and hematoxylin & eosin staining showed no visible alterations in kidney structure (Supplemental Figure 4, top). PAS staining showed few collapsed glomeruli with thickened glomeruli basement membrane in *Ctcf-cKO* mice (Supplementary Figure 4, middle). Also, we found a segmental and focal nodular expansion of the extracellular matrix in one kidney section from one *Ctcf-cKO* mouse (Supplementary Figure 4, middle). Masson trichrome evidenced small fibrotic areas in the interstitium and hypercellular glomeruli surrounded by a more intense collagen fiber staining in *Ctcf-cKO* mice than in control mice (Supplementary Figure 4, bottom). Renin immunostaining demonstrated many positive areas in *Ctcf-cKO* kidneys with a similar distribution found in the control group (Supplementary Figure 5A); however, the JG index revealed a 5% decreased in positive areas in the mutant mice (Supplementary Figure 5B). Measurements of the stained areas did not show a

significative difference between groups (data not shown). We also found a significant decreased in circulating renin (16,601 ± 5,645 *vs.* 25,819 ± 9,665 pg/mL) and in relative renin mRNA levels (0.689 ± 0.14 *vs.* 1.20 ± 0.15) of *Ctcf-cKO* mice when compared to control mice (Supplementary Figure 5C and D, respectively).

DISCUSSION

The present study shows that *Ctcf* is crucial for the maintenance of renin-expressing cells, kidney structure, and blood pressure/fluid homeostasis in adult mice. Because *Ctcf*-null mice are not viable[24], we generated conditional *Ctcf* knockout mice where *Ctcf* was deleted in cells from the renin lineage by crossing *Ctcf floxed* mice[11] with our mice expressing *Cre-recombinase* under the control of the endogenous $Ren1^{d}$ regulatory regions[12]. Loss of *Ctcf* in renin cells of mice at 4 months of age resulted in a severe depletion of renin-expressing cells with the attendant decrease in renin synthesis and release, decreased circulating renin and low blood pressure. Phenotypic changes were already present at 1 month of age and became more severe as the animals aged ultimately compromising kidney structure and function. Under the constant homeostatic threat of low blood pressure and fluid loss, the demands for renin increased over time leading to constant activation of the renin promoter driving the *Cre-recombinase* resulting in unremitting accumulation of *Ctcf* deletions and depletion of *Ctcf* along the arterial tree. In turn, the progressive lack of renin led to dehydration, inability to concentrate the urine, and widespread focal histological changes of tubular atrophy, sclerotic glomeruli, and interstitial fibrosis found at 2 months of age. The partial compensation at earlier stages may also be due to neogenesis of renin cells or recruitment of other cells to synthesize renin over time; however, as the deletions accumulate the number of cells expressing renin cannot be replenished.

In addition to a decreased in renin cell number, kidneys from *Ctcf-cKO* mice at 4 months of age showed additional abnormalities including reduced arteriolar branching of the kidney vasculature, tubular dilation, fibrosis and sclerotic glomeruli with abnormal Bowman's capsules. This phenotype resembles the phenotype seen in mice with deletion of *CBP* and *p300* also characterized by depletion of renin-expressing cells[14]. It also shares with such study the lack of concentric arteriolar hypertrophy consistently found in mice with deletion of any of the renin-angiotensin genes including the $Ren1^{c-/-}$ mice[25]. This suggests that the functions of *Ctcf* in renin cells extend beyond its influence on the renin gene and that the kidney abnormalities may not be due solely to the lack of renin. In the case of $Ren1^{c}$-KO mice, there is absolute lack of renin throughout life, but the endowment of renin null cells is not diminished as it occurs with double homozygous deletion of *Cbp/p300* or in *Ctcf-cKO* mice. Contrary to that, in $Ren1^{c}$-KO mice, cells of the renin lineage (even though they cannot produce renin) persist, increase in number throughout the kidney vasculature and retain the molecular program of the renin phenotype in a futile attempt to regain homeostasis[25]. Those overstimulated renin null cells retain embryonic characteristics and produce a variety of secreted growth factors that are likely to induce concentric vascular hypertrophy[25]. By the contrary, in *Ctcf* mice the endowment of renin-expressing cells is clearly diminished and the transcriptional machinery that governs the identity of the renin cells is compromised. It is therefore plausible that lacks of *Ctcf* completely distorts the ability of renin cells to maintain the molecular program that characterizes their phenotype,

thus explaining the lack of arteriolar hypertrophy heavily dependent on the presence of properly functioning overstimulated renin null cells. *Ctcf* mice displayed an arteriolar branching defect. We have previously shown that vascular renin is necessary for the proper morphogenesis (including branching and elongation) of the renal arterial tree[21]. It is therefore likely that the branching defect observed in our *Ctcf* mice is the result of the marked renin deficiency we encountered in the renal vasculature. These results are in keeping with the fundamental roles of *Ctcf* in chromatin structure including the establishment of large chromatin domains[5] and chromatin looping to regulate enhancer promoter interactions within topological associated domains where gene transcriptional activity occurs. Recently, Donlon and Morris[26] suggested the interesting possibility that *Ctcf* binding-sites serve as insulators of the *REN* human promoter in other cell types, preventing renin expression. As disruption of insulator's areas occurs in aging cells, genes may undergo inappropriate gene expression facilitated by its neighboring super-enhancers[26]. Further studies in our model will need to be performed to test this hypothesis. Further, it will be important to determine whether deletion of *Ctcf* caused changes in 3D chromatin organization of the renin cells and as a result altered renin cell fate. In this regard and as shown in Figure 1, we found that *Ctcf* has several conserved binding sites in renin cells within 40kb surrounding the *Ren1* locus and a binding site in the first intron of the renin gene. It could be possible that some of these sites are directly implicated in TAD formation as shown in the MCF-7 cell line[26]. It is therefore likely that the decreased number of renin-expressing cells, as a primary effect, could be due to lack of *Ctcf* binding to these sites in the proximity to the renin gene. Further studies may need to be performed to test whether specific deletion of those binding sites alters chromatin structure and renin cell fate.

In summary, *Ctcf* is necessary for the maintenance of renin cell identity and renin expression. Thus, we propose a model where mice lacking *Ctcf* in renin cells, develop severe kidney abnormalities and renal insufficiency throughout postnatal life. In normal renin cells, Ctcf might be part of the chromatin loop formation machinery required to bring into proximity crucial super-enhancers to their promoters. We suggest the distinct possibility that disruption of chromatin architecture in renin cells might be underlying our findings.

Supplementary Material

Refer to Web version on PubMed Central for supplementary material.

Acknowledgments

We thank Tiffany Southard, Fang Xu, Minghong Li, Rajwinderjit Kaur and Xiuyin Liang for technical assistance.

Funding: This work was funded by National Institutes of Health grants DK-096373 and DK-116718 to RAG, and DK-116196, DK-096373 and HL-148044 to MLSSL.

References

1. Gomez RA, Sequeira-Lopez MLS. Renin cells in homeostasis, regeneration and immune defence mechanisms. Nat Rev Nephrol. 2018;14:231 10.1038/nrneph.2017.186. [PubMed: 29380818]
2. Belyea BC, Santiago AE, Vasconez WA, et al. A primitive type of renin-expressing lymphocyte protects the organism against infections. bioRxiv. 1 2019:770511. doi:10.1101/770511

3. Gomez RA, Lynch KR, Chevalier RL, et al. Renin and angiotensinogen gene expression and intrarenal renin distribution during ACE inhibition. Am J Physiol Physiol. 1988;254(6):F900–F906. doi:10.1152/ajprenal.1988.254.6.F900
4. Martinez MF, Medrano S, Brown EA, et al. Super-enhancers maintain renin-expressing cell identity and memory to preserve multi-system homeostasis. J Clin Invest. 2018;128(11):4787–4803. doi:10.1172/JCI121361 [PubMed: 30130256]
5. Ong C-T, Corces VG. CTCF: an architectural protein bridging genome topology and function. Nat Rev Genet. 2014;15(4):234–246. doi:10.1038/nrg3663 [PubMed: 24614316]
6. Ohlsson R, Renkawitz R, Lobanenkov V. CTCF is a uniquely versatile transcription regulator linked to epigenetics and disease. Trends Genet. 2001;17(9):520–527. doi:10.1016/S0168-9525(01)02366-6 [PubMed: 11525835]
7. Chen H, Tian Y, Shu W, Bo X, Wang S. Comprehensive identification and annotation of cell type-specific and ubiquitous CTCF-binding sites in the human genome. PLoS One. 2012;7(7):e41374–e41374. doi:10.1371/journal.pone.0041374 [PubMed: 22829947]
8. Klenova EM, Nicolas RH, Paterson HF, et al. CTCF, a conserved nuclear factor required for optimal transcriptional activity of the chicken c-myc gene, is an 11-Zn-finger protein differentially expressed in multiple forms. Mol Cell Biol. 1993;13(12):7612–7624. https://www.ncbi.nlm.nih.gov/pubmed/8246978. [PubMed: 8246978]
9. Recillas-Targa F, Pikaart MJ, Burgess-Beusse B, et al. Position-effect protection and enhancer blocking by the chicken beta-globin insulator are separable activities. Proc Natl Acad Sci U S A. 2002;99(10):6883–6888. doi:10.1073/pnas.102179399 [PubMed: 12011446]
10. Guo Y, Xu Q, Canzio D, et al. CRISPR Inversion of CTCF Sites Alters Genome Topology and Enhancer/Promoter Function. Cell. 2015;162(4):900–910. doi:10.1016/j.cell.2015.07.038 [PubMed: 26276636]
11. Heath H, de Almeida CR, Sleutels F, et al. CTCF regulates cell cycle progression of αβ T cells in the thymus. EMBO J. 2008;27(21):2839–2850. doi:10.1038/emboj.2008.214 [PubMed: 18923423]
12. Sequeira López MLS, Pentz ES, Nomasa T, Smithies O, Gomez RA. Renin cells are precursors for multiple cell types that switch to the renin phenotype when homeostasis is threatened. Dev Cell. 2004;6(5):719–728. doi:10.1016/S1534-5807(04)00134-0 [PubMed: 15130496]
13. Sigmund CD, Okuyama K, Ingelfinger J, et al. Isolation and characterization of renin-expressing cell lines from transgenic mice containing a renin-promoter viral oncogene fusion construct. J Biol Chem. 1990.
14. Gomez RA, Pentz ES, Jin X, Cordaillat M, Sequeira Lopez MLS. CBP and p300 are essential for renin cell identity and morphological integrity of the kidney. AJP Hear Circ Physiol. 2009;296(5):H1255–H1262. doi:10.1152/ajpheart.01266.2008
15. Sequeira-Lopez MLS, Weatherford ET, Borges GR, et al. The MicroRNA-Processing Enzyme Dicer Maintains Juxtaglomerular Cells. J Am Soc Nephrol . 2010;21(3):460–467. doi:10.1681/ASN.2009090964 [PubMed: 20056748]
16. Sequeira Lopez ML, Pentz ES, Robert B, Abrahamson DR, Gomez RA. Embryonic origin and lineage of juxtaglomerular cells. Am J Physiol Renal Physiol. 2001;281(2):F345–56. http://ajprenal.physiology.org/content/281/2/F345.abstract. Accessed January 14, 2017. [PubMed: 11457727]
17. Lin EE, Sequeira-Lopez MLS, Gomez RA. RBP-J in FOXD1+ renal stromal progenitors is crucial for the proper development and assembly of the kidney vasculature and glomerular mesangial cells. Am J Physiol - Ren Physiol. 2014;306(2):F249–F258. doi:10.1152/ajprenal.00313.2013
18. Pentz ES, Cordaillat M, Carretero OA, Tucker AE, Sequeira Lopez MLS, Gomez RA. Histone acetyl transferases CBP and p300 are necessary for maintenance of renin cell identity and transformation of smooth muscle cells to the renin phenotype. AJP Hear Circ Physiol. 2012;302(12):H2545–H2552. doi:10.1152/ajpheart.00782.2011
19. Pentz ES, Moyano MA, Thornhill BA, Sequeira Lopez MLS, Gomez RA. Ablation of renin-expressing juxtaglomerular cells results in a distinct kidney phenotype. Am J Physiol Integr Comp Physiol. 2004;286(3):R474–R483. doi:10.1152/ajpregu.00426.2003

20. Pentz ES, Lopez, KIM H-S, CARRETERO O, SMITHIES O, GOMEZ RA. Ren1d and Ren2 cooperate to preserve homeostasis: evidence from mice expressing GFP in place of Ren1d. Physiol Genomics. 2001;6(1):45–55. doi:10.1152/physiolgenomics.2001.6.1.45 [PubMed: 11395546]

21. Reddi V, Zaglul A, Pentz ES, Gomez RA. Renin-expressing cells are associated with branching of the developing kidney vasculature. J Am Soc Nephrol. 1998;9(1):63 LP - 71. http://jasn.asnjournals.org/content/9/1/63.abstract. [PubMed: 9440088]

22. Nagalakshmi VK, Li M, Shah S, et al. Changes in cell fate determine the regenerative and functional capacity of the developing kidney before and after release of obstruction. Clin Sci. 2018;132(23):2519 LP - 2545. doi:10.1042/CS20180623

23. Davis CA, Hitz BC, Sloan CA, et al. The Encyclopedia of DNA elements (ENCODE): data portal update. Nucleic Acids Res. 2018;46(D1):D794–D801. doi:10.1093/nar/gkx1081 [PubMed: 29126249]

24. Fedoriw AM, Stein P, Svoboda P, Schultz RM, Bartolomei MS. Transgenic RNAi Reveals Essential Function for CTCF in *H19* Gene Imprinting. Science (80-). 2004;303(5655):238 LP - 240. http://science.sciencemag.org/content/303/5655/238.abstract.

25. Oka M, Medrano S, Sequeira-López MLS, Gómez RA. Chronic Stimulation of Renin Cells Leads to Vascular Pathology. Hypertension. 2017;70(1):119 LP - 128. http://hyper.ahajournals.org/content/70/1/119.abstract. [PubMed: 28533331]

26. Donlon TA & Morris B In silico analysis of human renin gene–gene interactions and neighborhood topologically associated domains suggests breakdown of insulators contribute to ageing-associated diseases. Biogerontology. 2019:pp 1–13. doi:10.1007/s10522-019-09834-1

Clinical Perspectives

- Experimental deletion of *Ctcf* in cells from the renin lineage led to a model of kidney fibrosis an end stage renal disease.
- Lack of *Ctcf* leads to decreased endowment of renin-expressing cells accompanied by decreased circulating renin, hypotension, severe morphological abnormalities of the kidney, including arteriolar branching defect, and ultimately renal failure.
- Understanding the role of key regulators involved in renin expression and renin lineage cell identity may be of benefit for the management of patients with blood pressure disorders and renal diseases.

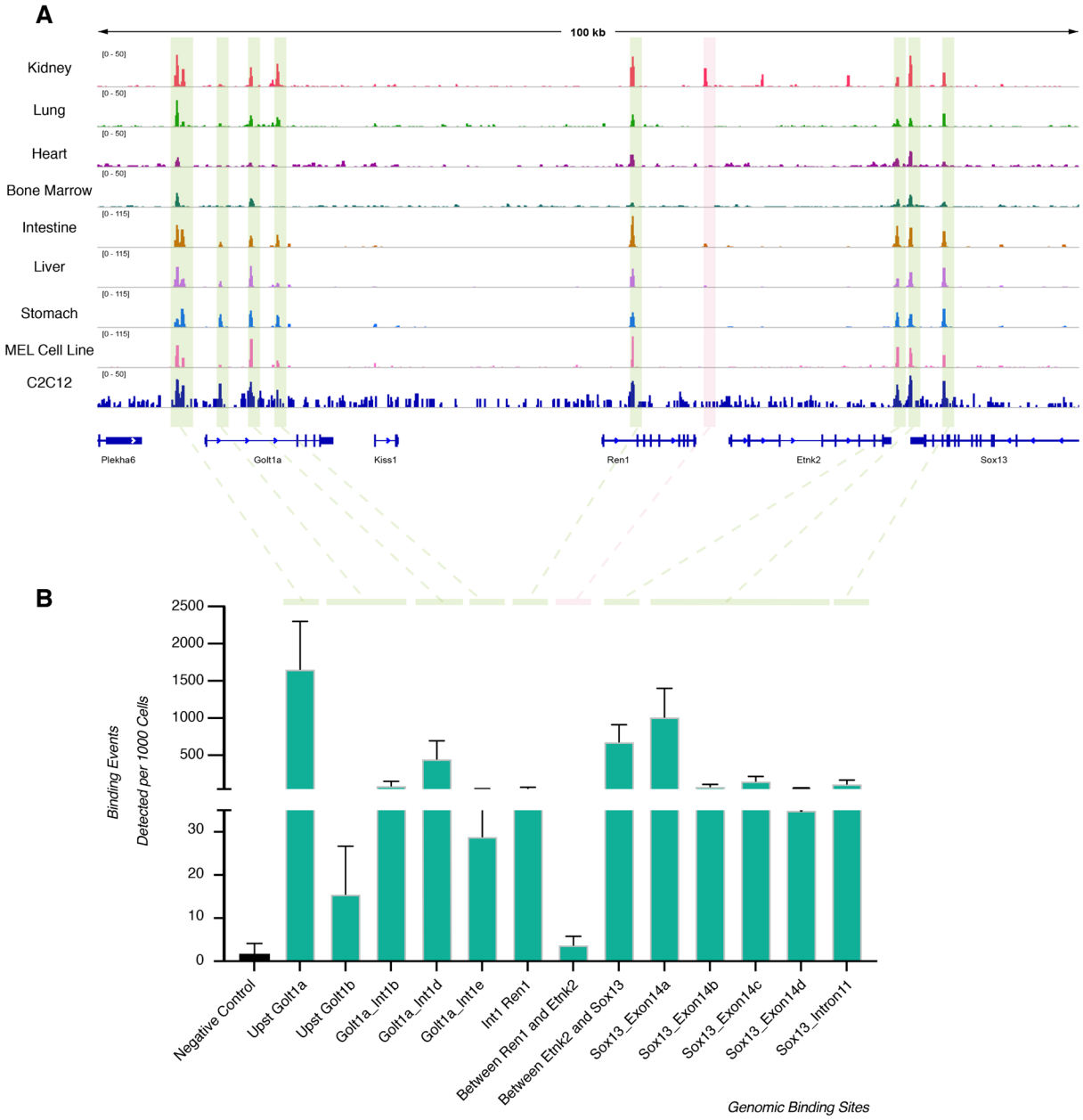

Figure 1. Ctcf binding at the Ren1 locus.

A. Genome browser image shows that *Ctcf* binds in the neighborhood and within intron 1 of the *Ren1* gene in different mouse tissues and cell types. **B.** ChIP-qPCR for *Ctcf* binding sites in As4.1 cells. The histogram presents the immunoprecipitated DNA fragments amplified by quantitative real-time PCR. Bars represent the mean ± SD (n=3). Green dashed lines: areas of *Ctcf binding* coinciding in both panels; pink dashed line: indicates the *Ctcf* binding region in the kidney sample that is not enriched in the ChIP-seq samples or in the ChIP-qPCR from As4.1 cells.

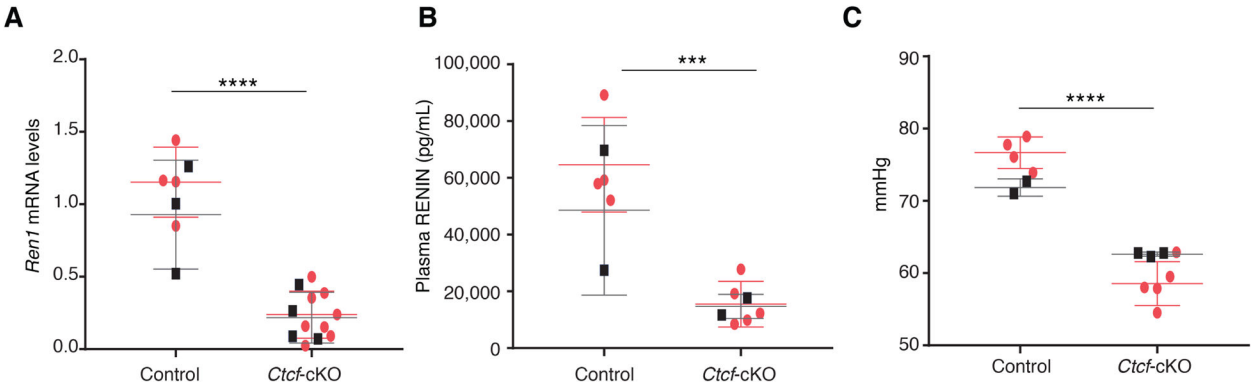

Figure 2. Deletion of *Ctcf* in renin cells causes a decrease in renin mRNA levels, circulating renin, and arterial blood pressure.

A. Renin mRNA levels were markedly reduced in *Ctcf-cKO* mice (n=12) in comparison to control mice (n=7). **B.** *Ctcf-cKO* mice (n=7) showed a significant decreased in plasma renin levels compared to control mice (n=6). **C.** *Ctcf-cKO* mice (n=8) were hypotensive when compared to control mice (n=6). Data are presented as Mean ± SD. ****p<0. 001, ****p<0.0001,* by unpaired, 2-sided Student's *t*-test. Black squares, males; red dots, females.

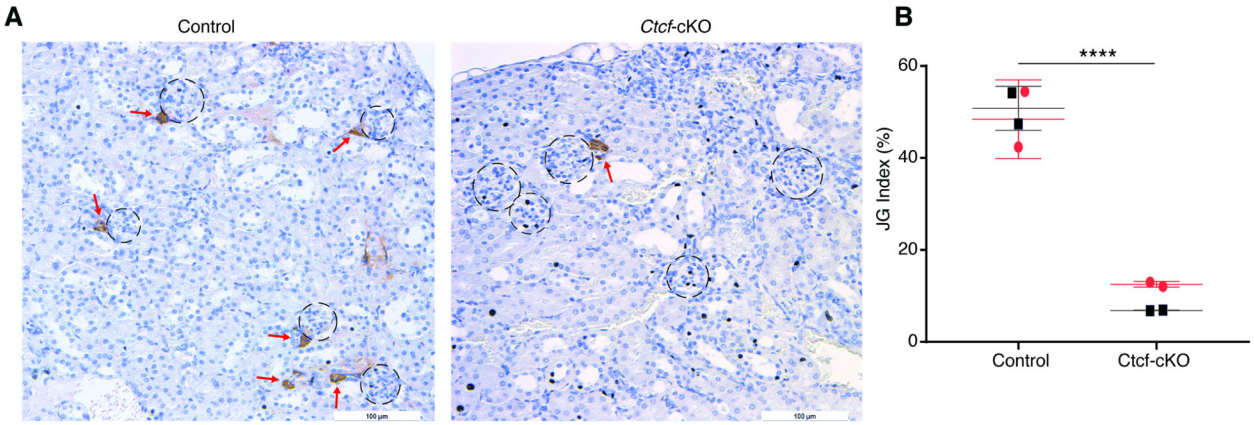

Figure 3. Deletion of *Ctcf* causes severe depletion of renin cells.

A. Immunohistochemistry for renin shows the normal renin distribution (brown, red arrows) at the entrance of the glomeruli in control kidneys (Left) whereas a marked decrease in renin distribution and storage is seen in kidneys of *Ctcf*-cKO mice (Right). Circles indicate glomeruli. **B.** JG index is markedly reduced in *Ctcf*-cKO mice (n=4) when compared to control mice (n=4). Data are presented as mean ± SD. ****p<0. 0001,* by unpaired, 2-sided Student's *t*-test. Black squares, males; red dots, females.

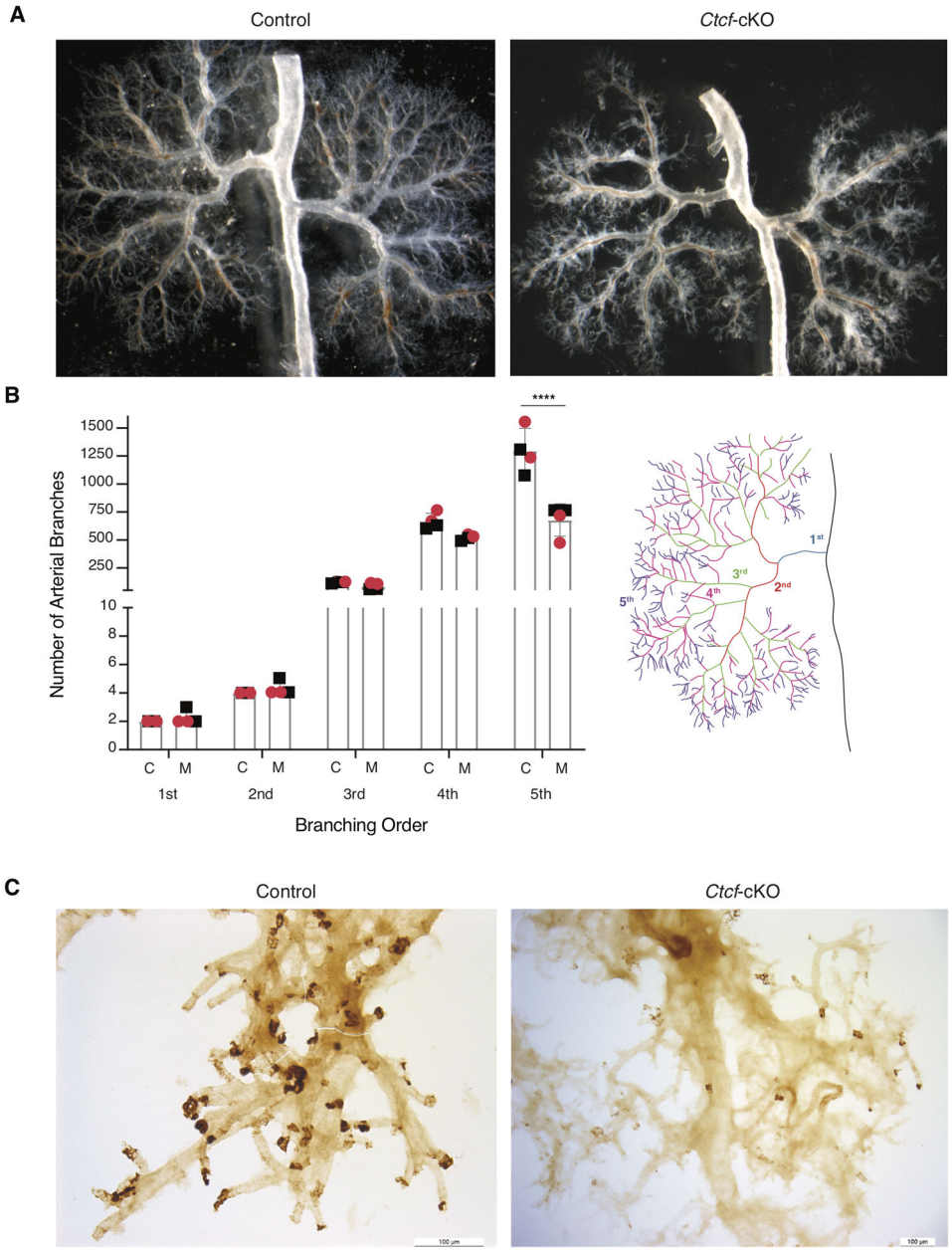

Figure 4. Deletion of *Ctcf* affects the branching pattern of the renal arterial tree.

A. Renal arterial tree of control mice (left) and *Ctcf*-cKO mice (right) at 4 months of age. **B.** Left. The histogram shows that mutant mice (n=4) show fewer smaller branches of the 5th order than control mice (n=4). Data are presented as mean ± SD. * ****p<0.0001*, by 2-way ANOVA, using Sidak's multiple comparisons test. Right. Scheme showing the branching order (from 1st to 5th). Black squares, males; red dots, females; C, Control group; M, Mutant group **C.** Renin immunolocalization (brown) in microdissected arterial trees show fewer and also lighter renin positive spots at the tip of afferent arterioles in *Ctcf*-cKO mice than in control mice.

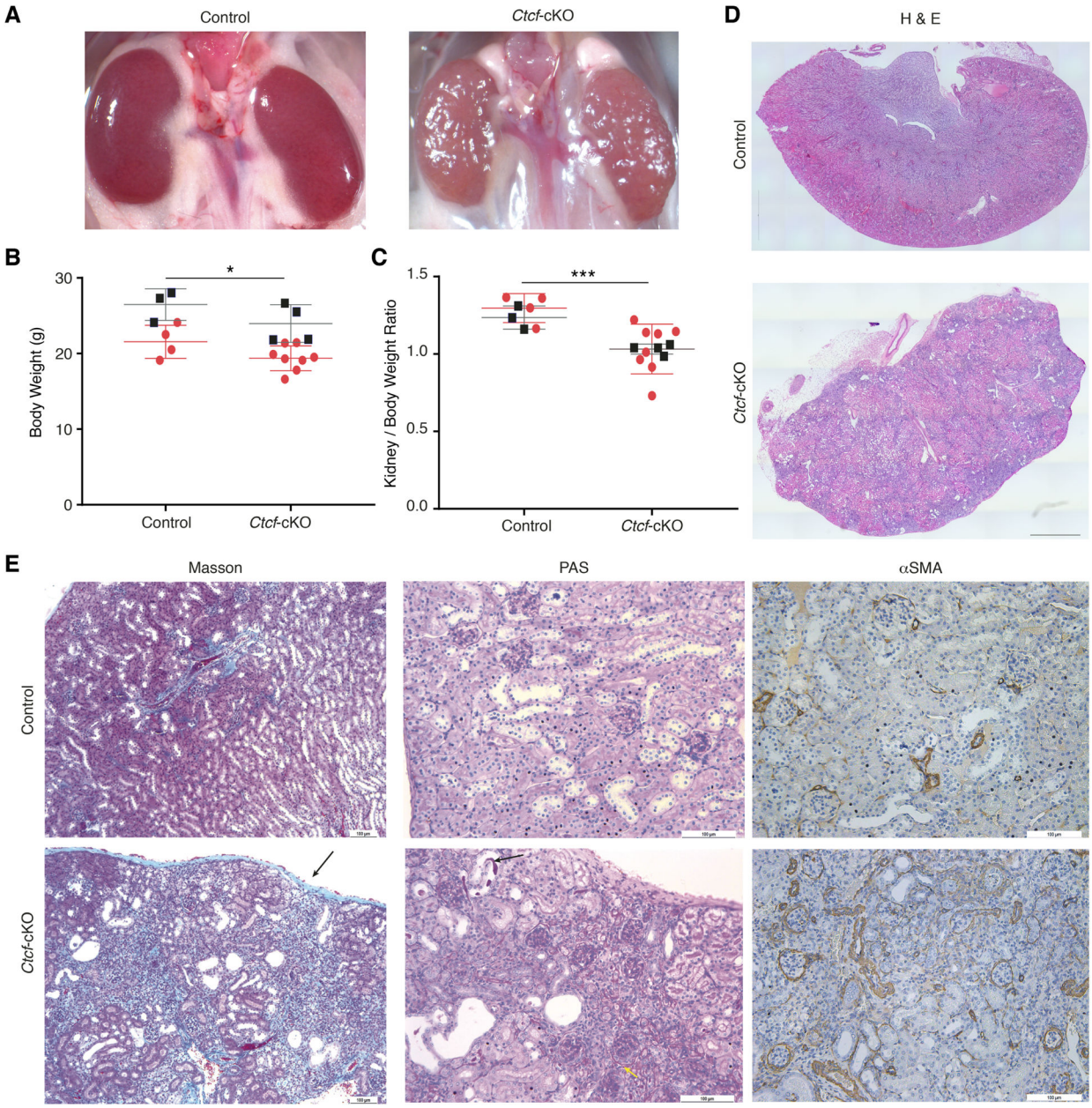

Figure 5. Deletion of *Ctcf* affects somatic and kidney growth and leads to severe kidney abnormalities.

A. Kidneys from *Ctcf-cKO* mice are small, pale, and with irregular surfaces. **B.** Body weights of *Ctcf-cKO* mice (n=12) were significantly lower than in control animals (n=7). **C.** The kidney/body weight ratio was markedly decreased in *Ctcf-cKO* mice. **D.** A tiled image of H&E staining reveals disorganized kidney structure, lack of cortical-medullary junctions, and dilated tubules in kidneys from *Ctcf-cKO* mice (bottom). **E.** Left, Masson's trichrome shows interstitial fibrosis (blue) with cortical depressions (arrow) in *Ctcf-cKO* kidneys. Also, peri and intraglomerular fibrosis are observed. Middle, PAS staining indicates intraluminal casts in dilated tubules (black arrows) and sclerotic glomeruli with fibrocellular crescent formation (yellow arrow) surrounded by disorganized packed cells. Right, αSMA

immunostaining shows an increased expression of αSMA in the interstitium, around and within glomeruli. Quantitative data are presented as mean ± SD. *$p<0.05$, ***$p<0.001$, by unpaired, 2-sided Student's *t*-test. Black squares, males; red dots, females.

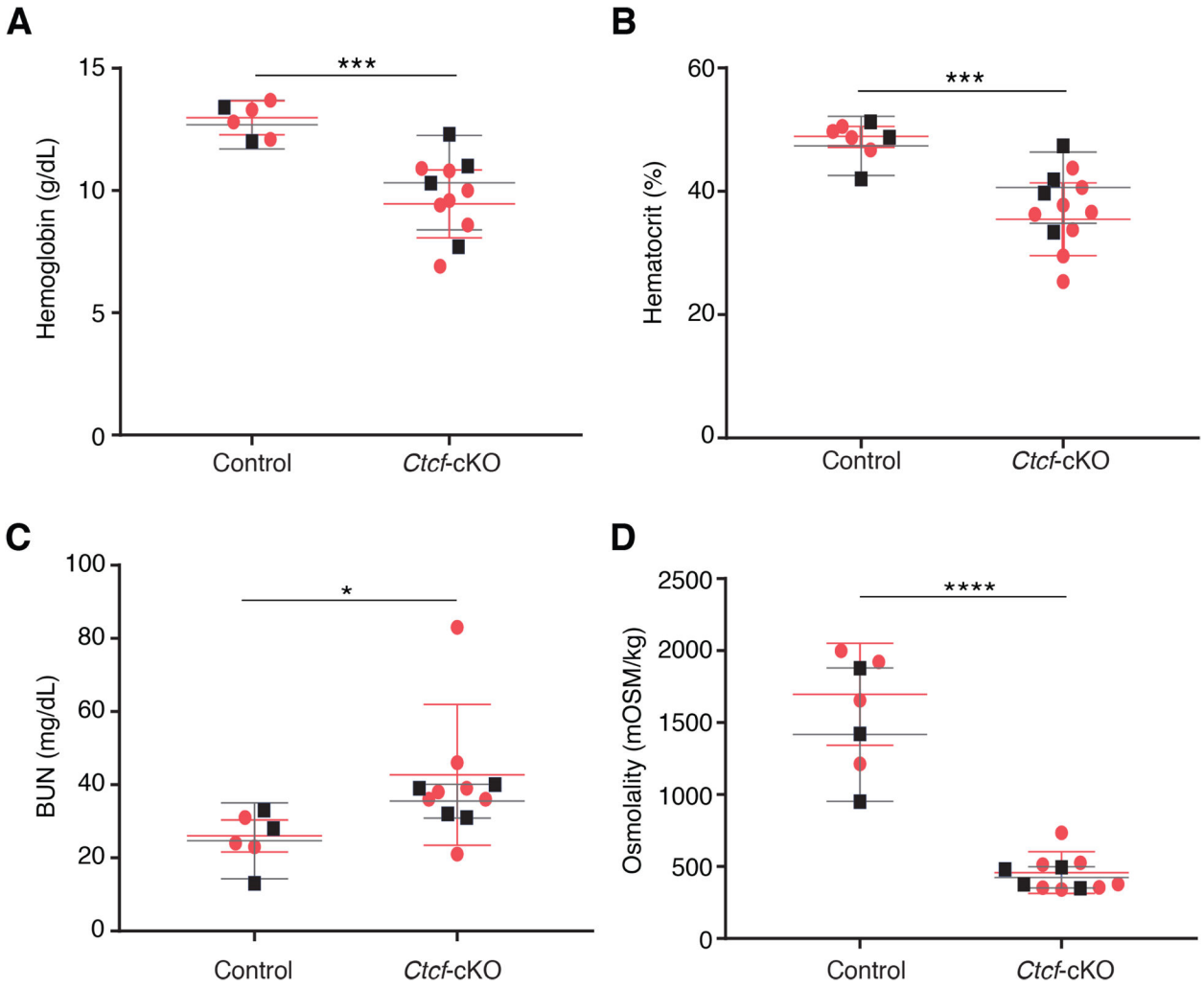

Figure 6. Deletion of *Ctcf* causes anemia and renal failure.

Ctcf-cKO mice shows anemia characterized by low hemoglobin (**A.** *Ctcf-cKO*, n= 11; Control, n= 6) and low hematocrit (**B.** *Ctcf-cKO*, n= 12; Control, n= 7)**. C.** The blood urea nitrogen was significantly increased in *Ctcf-cKO* mice (n=11) compared to control mice (n=6), indicating renal failure. **D.** Measurement of urine osmolality indicated that *Ctcf-cKO* mice (n=11) cannot concentrate their urine. Mean ± SD. *$p<0.05$, ***$p<0.001$, ****$p<0.0001$, unpaired, 2-sided Student's *t* test. Black squares, males; red dots, females.